Multi-Objective Optimization of Departure Procedures at Gimpo International Airport

Junghyun Kim[1], Dongwook Lim, Dylan Jonathan Monteiro, Michelle Kirby, Dimitri Mavris[2]

Aerospace Systems Design Lab., Georgia Institute of Technology, Atlanta, Georgia, United States

Abstract

Most aviation communities have increasing concerns about the environmental impacts, which are directly linked to health issues for local residents near the airport. In this study, the environmental impact of different departure procedures using the Aviation Environmental Design Tool (AEDT) was analyzed. First, actual operational data were compiled at Gimpo International Airport (March 20, 2017) from an open source. Two modifications were made in the AEDT to model the operational circumstances better and the preliminary AEDT simulations were performed according to the acquired operational procedures. Simulated noise results showed good agreements with noise measurement data at specific locations. Second, a multi-objective optimization of departure procedures was performed for the Boeing 737-800. Four design variables were selected and AEDT was linked to a variety of advanced design methods. The results showed that takeoff thrust had the greatest influence and it was found that fuel burn and noise had an inverse relationship. Two points representing each fuel burn and noise optimum on the Pareto front were parsed and run in AEDT to compare with the baseline. The results showed that the noise optimum case reduced Sound Exposure Level (SEL) 80-dB noise exposure area by approximately 5% while the fuel burn optimum case reduced total fuel burn by 1% relative to the baseline for aircraft-level analysis.

Keywords: Aviation Environmental Design Tool (AEDT), Multi-objective Optimization, Airport Noise

1. Introduction

Researches on aircraft noise and its health effects are growing rapidly worldwide and there have been many important findings published in recent years. For example, the Civil Aviation Authority (CAA) published a report that examined the evidence related to aircraft noise and the resulting impacts on various health problems. [1] In addition, the World Health Organization (WHO) published their Burden of Disease from Environmental Noise report, which indicated healthy life years lost due to environmental noise. [2]

Nevertheless, aviation traffic continues to grow, primarily due to world economic growth. According to their annual report in 2017, the Federal Aviation Administration (FAA) projects U.S. carrier passenger growth over the next 20 years to average 1.9 percent per year. [3] Moreover, the International Air Transport Association (IATA) forecasts 7.2 billion passengers will travel by air in 2035, which is 3.7 billion more than today. [4]

[1] Ph. D. Student, First author: andy.kim@gatech.edu
[2] Regent Professor, Corresponding author: dimitri.mavris@aerospace.gatech.edu

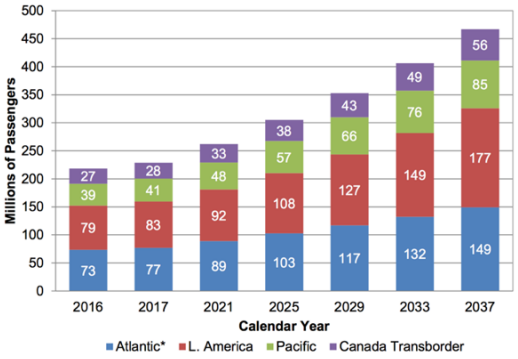

Fig. 1. Total Passengers to/from the U.S. [3]

In response to these concerns, a few of strategies have been adopted in order to reduce the community noise impacts: 1) Restricting the number of operations, 2) Phasing out noisier aircraft, 3) Land use and airport planning, 4) Developing noise-reduction aircraft and engine technologies, 5) Considering optimized flight tracks for noise reduction, and 6) Establishing different flight procedures/trajectories.

In this study, an investigation was conducted on different departure procedures using AEDT which has been developed by the FAA to assess the environmental effects of aviation. [10]

2. Research Motivation

In 1993, the FAA issued Advisory Circular (AC) 91-53A that described two standard noise abatement departure procedures (NADP-1 and NADP-2) to minimize noise impact for subsonic turbo-jet aircraft with Takeoff Gross Weight (TOGW) more than 75,000 lbs. [5] According to AC91-53A, NADP-1 is intended to provide noise reduction for areas close to airport; whereas, NADP-2 is designed to provide noise reduction for areas more distant to the runway end.

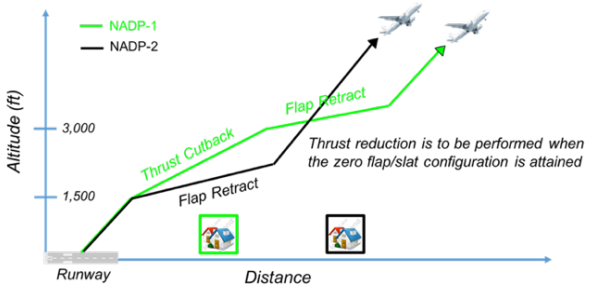

Fig. 2. Noise Abatement Departure Procedures (NADP)

To be more specific, NADP-1, which is called as Close-in NADP, initiates thrust cutback at an altitude of no less than 800 feet. On reaching an altitude above 800 feet, the procedure reduces engine thrust and flies with flaps and slats in the takeoff configuration. At an altitude equivalent to 3,000 feet, it accelerates and retracts flaps and slats to normal climb speed on schedule. On the other hand, in NADP-2 which is called as Distant NADP, the flap and slats are to be retracted first and the thrust cutback is to be performed when the zero flap and slat configuration is attained.

Although the FAA allows the airlines to adopt up to two noise abatement departure procedures to minimize noise impact, it was observed by several research studies that the procedures customized for specific airport may offer greater noise reduction benefits because the surrounding residential areas nearby the airport are different from each other. For instance, J.P. Clarke from Georgia Institute of Technology optimized profile descent arrivals at Los Angeles International Airport [20], designed continuous descent approach for Louisville international Airport [21], and evaluated noise abatement procedures at Boston's Logan airport. [6] Based on these papers, he claimed that the benefits of noise abatement departures and arrivals are specific. Moreover, H.G. Visser from Delft University of Technology combined INM (Integrated Noise Model), Geographic systems, and optimization algorithms into a single tool to develop a NADP for only Amsterdam airport. [7] Also, Tom G. Reynolds from University of Cambride worked with J.P. Clarke to develop and analyze noise abatement procedures for UK airports. [22] For this research, Gimpo International Airport (RKSS), one of international airports in South Korea, was selected to study environmental impacts around the airport.

In 2003, the Korean government announced that all airlines operating at Gimpo International Airport must use NADP-1 for noise abatement purpose. [8] Furthermore, the government specified areas where noise exposure level is higher than 75 Weighted Equivalent Continuous

Perceived Noise Level (WECPNL) and established a policy [12] for residents living around the area as shown in Figure 3.

Although most countries over the world have not used the WECPNL, some Asian countries including South Korea do. In Figure 3, the Korean government divided two regions for different noise countermeasure policy: 1) An area in red solid line is directly influenced by aircraft noise higher than 75 WECPNL and 2) An area in blue solid line is not influenced by 75 WECPNL; however, the area is still influenced by aircraft noise.

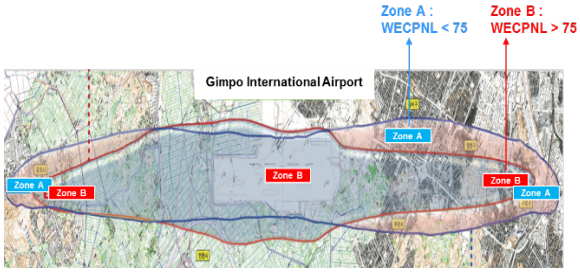

Fig. 3. Noise countermeasure policy on Gimpo International Airport in 2012 (Korea Airport Corporation) [14]

Since the INM has been replaced by AEDT as of May 2015 [9], it seems that the noise exposure areas in Figure 3 must have been generated by INM. However, both INM and AEDT have been developed with a few of assumptions which lead to some discrepancies between simulation results and the reality. For instance, both AEDT and INM assume 100% maximum takeoff thrust in simulation; whereas, FAA provided guidance for use of Reduced Thrust Takeoff (RTT) to save maintenance cost and to increase engine life. [17] Furthermore, most airlines and airports prefer to use NADP-2 procedures [19]; whereas only ICAO-A (International Civil Aviation Organization), ICAO-B, and Standard procedures are available in AEDT and INM. In addition, both AEDT and INM use an assumption of 65% of maximum structural payload capacity and fuel weight based on the stage length because it is hard to collect the real data on aircraft departure weight; whereas, the reality has specific weight information because aircraft departure weight varies with the change in number of passengers and the amount of fuel carried by an aircraft. [10]

Hence, in order to reduce the gap between simulation results generated by INM/AEDT and the reality, it would be highly recommended to adjust the assumptions and to model a RTT and NADP in INM/AEDT. In this study, these assumptions were modified and simulated in AEDT, as discussed in detail in the following section.

3. Verification and Validation (V&V)

3.1 Compiling real flight data

In order to compare simulation results with the noise measurement data, the real flight operations on March 20, 2017 at Gimpo International Airport were compiled from commercially open source data. First, the data such as flight number was obtained from the Korean government website. Using the flight number, an investigation of flight radar track information through the Flight-Aware website was performed. In addition, the takeoff and landing runway assignment information was obtained from the Aeronautical Information Publication (AIP) of Republic of Korea [11] and Google Earth software program.

Subsequently, both departure and arrival schedules for March 20, 2017 at Gimpo International Airport were reproduced for validation purposes. The flight schedule included 12 airlines, 11 unique aircraft types, and total 398 operations (198 departures and 200 arrivals) from 06:19 a.m. to 10:47 p.m. as listed in Table 1.

Table 1. Flight schedule on March 20, 2017 at Gimpo International Airport (Departure)

#	Airline	Flight	Aircraft Type	Itinerary (To)	Runway	Time	Operation	Type	Stage Length	Track #	Status
1	Asiana Airlines	OZ8901	Airbus A320 (twin-jet)	CJU(제주)	14L	6:19	1	Civil	1	1	Departure
2	Asiana Airlines	OZ8905	Airbus A321 (twin-jet)	CJU(제주)	14L	6:25	1	Civil	1	1	Departure
3	Tway Airlines	TW751	Boeing 737-800 (twin-jet)	CJU(제주)	14L	6:35	1	Civil	1	1	Departure
4	Eastar Jet	ZE201	Boeing 737-800 (twin-jet)	CJU(제주)	14L	6:38	1	Civil	1	1	Departure
5	Jin Air	LJ301	Boeing 737-800 (twin-jet)	CJU(제주)	14L	6:41	1	Civil	1	1	Departure
6	Jin Air	LJ303	Boeing 737-800 (twin-jet)	CJU(제주)	14L	6:51	1	Civil	1	1	Departure
7	Jeju Air	7C101	Boeing 737-800 (twin-jet)	CJU(제주)	14L	6:53	1	Civil	1	1	Departure
8	Asiana Airlines	OZ8907	Airbus A321 (twin-jet)	CJU(제주)	14L	6:56	1	Civil	1	1	Departure
9	Korean Air	KE1201	Boeing 737-900 (twin-jet)	CJU(제주)	14L	7:02	1	Civil	1	1	Departure
10	Korean Air	KE1603	Boeing 737-800 (twin-jet)	USN(울산)	14L	7:08	1	Civil	1	12	Departure
11	Tway Airlines	TW761	Boeing 737-800 (twin-jet)	CJU(제주)	14L	7:11	1	Civil	1	1	Departure
12	Korean Air	KE1101	Boeing 737-800 (twin-jet)	PUS(김해)	14L	7:13	1	Civil	1	8	Departure
13	Air Busan	BX8011	Airbus A321 (twin-jet)	CJU(제주)	14L	7:16	1	Civil	1	1	Departure
14	Asiana Airlines	OZ8731	Airbus A321 (twin-jet)	RSU(여수)	14L	7:18	1	Civil	1	9	Departure
15	Korean Air	KE1631	Boeing 737-800 (twin-jet)	HIN(사천)	14L	7:21	1	Civil	1	2	Departure
16	Tway Airlines	TW701	Boeing 737-800 (twin-jet)	CJU(제주)	14L	7:23	1	Civil	1	1	Departure
17	Jeju Air	7C103	Boeing 737-800 (twin-jet)	CJU(제주)	14L	7:26	1	Civil	1	1	Departure
18	Jeju Air	7C151	Boeing 737-800 (twin-jet)	CJU(제주)	14L	7:29	1	Civil	1	1	Departure
19	Eastar Jet	ZE203	Boeing 737-700 (twin-jet)	CJU(제주)	14L	7:31	1	Civil	1	1	Departure
20	Asiana Airlines	OZ8981	Boeing 767-300 (twin-jet)	CJU(제주)	14L	7:35	1	Civil	1	1	Departure
21	Air Busan	BX8013	Airbus A321 (twin-jet)	CJU(제주)	14L	7:37	1	Civil	1	1	Departure
22	Air Busan	BX8803	Airbus A320 (twin-jet)	PUS(김해)	14L	7:42	1	Civil	1	8	Departure
23	Asiana Airlines	OZ8703	Airbus A320 (twin-jet)	KWJ(광주)	14L	7:52	1	Civil	1	6	Departure
24	Asiana Airlines	OZ8909	Airbus A320 (twin-jet)	CJU(제주)	14L	7:54	1	Civil	1	1	Departure
25	Jeju Air	7C105	Boeing 737-800 (twin-jet)	CJU(제주)	14L	8:04	1	Civil	1	1	Departure
26	JAL	JL90	Boeing 767-300 (twin-jet)	HND(하네다)	14L	8:08	1	Civil	1	3	Departure

3.2. Reduced Thrust Takeoff (RTT) Modeling

Most airlines have implemented a RTT because of the many benefits such as decrease in maintenance cost and increase in engine life. Unfortunately, AEDT/INM does not model the RTT but rather uses 100% maximum takeoff thrust. To ensure realistic results, the RTT was modeled by changing regression coefficients in the Jet Rated Thrust equation as shown in Equation (1), specifically coefficient E.

$$\frac{F_n}{\delta} = E + F \cdot v + G_A \cdot h + G_B \cdot h^2 + H \cdot T_C \qquad (1)$$

$$T_C = Temperature\ at\ the\ aircraft\ (℃)$$
$$E, F, G_A, G_B, H = Regression\ coefficients$$
$$v = Calibrated\ airspeed\ (kt)$$
$$h = Altitude\ MSL\ (ft)$$
$$F_n/\delta = Corrected\ net\ thrust\ per\ engine\ (lbf)$$

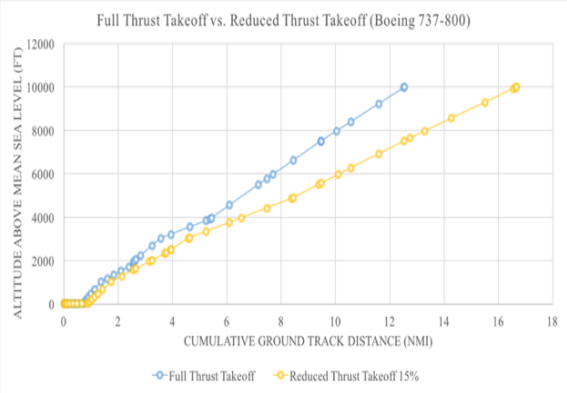

Fig. 4. Flight trajectory (Full thrust vs. RTT)

3.3. NADP Modeling

The FAA's AC91-53A provided two departure procedures (Close-in and Distant) in 1993 to aircraft operators to mitigate noise impacts on communities. In 1996, the Air Line Pilots Association (ALPA) formally supported the policy. Since AIP Republic of Korea and RKSS AD 2.21 recommends that all departing aircraft should apply NADP-1 with thrust reduction at 1,000 feet [11], the NADP-1 for a Boeing 737-800 (the aircraft with the largest percentage of operations on March 20, 2017) was modeled in AEDT.

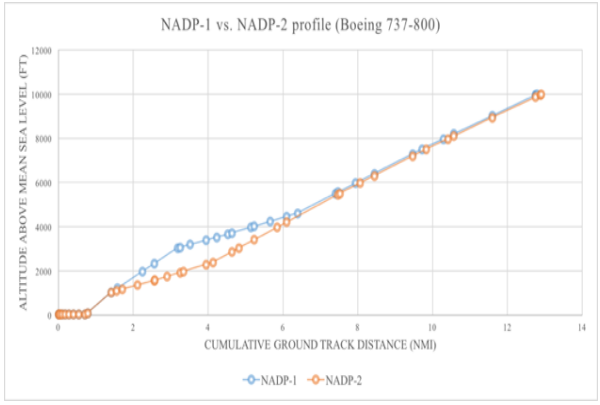

Fig. 5. NADP-1 modeling in AEDT

For NADP modeling, coefficients for Flap 01 of Boeing 737-800 were calculated with the reference conditions because RTT procedures are typically flown with Flap 01 instead of Flap 05 (AEDT only defines Flap 05 for Boeing 737-800) Furthermore, the energy-share method (Step type: P) was used for NADP modeling instead of standard procedure definition method with average rate of climb and final calibrated airspeed (Step type: A). This is because of one major benefit of the energy-share method such that the acceleration percentage is constant for each stage-length which refers to the length/distance traveled by aircraft from takeoff to landing; whereas, the standard procedure definition method requires unique parameters for each stage-length. For instance, instead of explicitly specifying rate of climb for the acceleration steps, the energy-share method specifies a percentage of thrust applied to horizontal acceleration and this is used to calculate the dimensionless climb gradient for the acceleration phases.

3.4. Atmospheric Absorption Model

In both INM and AEDT, it is important to choose an atmospheric absorption model to properly model the manner in which the noise attenuates over distance, as this can greatly impact the size of the noise exposure area. For INM, two atmospheric absorption models are available: 1) SAE-AIR-1845 and 2) SAE-ARP-866A. To be specific, SAE-AIR-1845 uses the Noise-Power-Distance (NPD) data without any

adjustment for standard air; whereas, SAE-ARP-866A adjusts NPD data for specified temperature and humidity. For AEDT, an additional model is included, namely SAE-ARP-5534, which adjusts NPD for specified temperature, humidity, and pressure.

In this study, airport weather information on March 20, 2017 at Gimpo International Airport was investigated from the website of the Korean Aviation Meteorological Office and the SAE-ARP-5534 atmospheric absorption model was used for the simulation.

3.5. Grid Resolution Study

In order to assess the computational costs associated with the noise grid resolution, a study was performed with increasing grid density. All seven levels were run at Gimpo International Airport until the 75 WECPNL noise contour area converged. Finally, 268,800 grid points with a 0.0625 nautical mile spacing was chosen for the simulation based on a balance of speed versus accuracy.

Table 2. Grid resolution study

Total grid points	X count	Y count	Spacing (nmi)	Execution time (sec)	WECPNL 75 area (km^2)
1,050	35	30	1.000	15	4.92
4,200	70	60	0.500	33	7.96
16,800	140	120	0.250	109	9.96
67,200	280	240	0.125	373	9.97
268,800	560	480	0.062	1,503	9.98
1,075,200	1,120	960	0.031	6,000	9.98
4,300,800	2,240	1,920	0.015	17,142	9.98

3.6. Validation on Noise measurement data

In summary, the following computational setup was used in the simulation to reduce the gap between AEDT and the real world operations: 1) 15% Reduced Thrust Takeoff, 2) Noise Abatement Departure Procedure-1 with thrust cutback at 1,000 feet, 3) Energy-share method and Flaps 01 takeoff flap setting, and 4) SAE-ARP-5534 atmospheric absorption model. Based on the computational setup, the accuracy of the simulation was validated for WECPNL values by comparing against the noise measurement data.

Table 3. Simulation vs. Measurement data at the specific locations

Measurement Location	WECPNL (Simulation)	WECPNL (Measurement)
Gogang Elem. School	72.0	72.1
Shinnam Elem. School	75.7	74.4
Gogang Apartment	83.4	81.7
Shinwon Elem. School	75.4	75.0
Gocheok Midd. School	74.0	74.7

As evident in Table 3, the results show good agreement overall; however, small differences still exist between simulation and measurement. The sources of these discrepancies include: 1) A measurement location could not be exactly matched, and 2) WECPNL (Measurement) was calculated slightly different [12] to ICAO definition of WECPNL (AEDT).

4. Multi-Objective Optimization

4.1. Operational Variables

For this case study, a few operational variables associated with Boeing 737-800 NADP-1 were explored because of two reasons: 1) Boeing 737-800 was aircraft with the largest percent operations at Gimpo International Airport. 2) All airlines operating at Gimpo International Airport must use NADP-1 for noise abatement purpose. Four variables were finally chosen for Boeing 737-800 NADP-1: Takeoff thrust, Cutback altitude, Acceleration altitude, and Percent of horizontal acceleration in the energy-shared method. In order to ensure safety issues, the four operational variable ranges were determined by referring the FAA Advisory Circular (AC) 91-53. FAA AC91-53 provides criteria for acceptable NADPs to ensure safe operation. For instance, it sets the lower limit for thrust cutback altitude at 800 feet. It also specifies that the speed should not decrease to less than V_2 and the engine thrust level should be sufficient to maintain at least zero percent climb gradient in the case of one engine failure. The lower and upper bounds for the four design variables were selected to ensure that the developed departure procedures meet these

criteria. Design variables and ranges are tabulated in Table 4.

Table 4. Design variables and ranges

Description	Lower bound	Baseline	Upper bound	Unit
Takeoff Thrust	22175.7	22175.7	26089.1	lbf
Cutback Altitude	800	1000	1500	ft
Acc. Altitude	2700	3000	3300	ft
Horizontal Acc.	49.5	55	60.5	%

4.2. Design of Experiments (DoE)

A DoE is defined as a procedure that selects a set of samples in the design space in order to maximize the amount of information with a limited set of experiments. In this study, both Central Composite Design (CCD) and Latin Hypercube Sampling (LHS) were combined to generate hybrid DoE tables. CCD is one of the most commonly used structured-DoE methods because it is designed to capture corner points of design space; whereas, it is hard to capture inner points which are especially important to this study. On the other hand, LHS is well-developed to capture inner points and non-linearity of design space; however, it is not well-formulated to capture the corner points. In order to capture both boundary and interior points of design space, 25 points which were calculated by the Equation (2) were allocated for CCD and 50 points were specified for LHS. For total 75 sample points, the design variables for the Boeing 737-800 were modified with lower/upper bounds and AEDT was run to generate results for fitting a surrogate model.

$$2^n + 2n + 1 \quad (2)$$

4.3. Surrogate Modeling

In general, a surrogate model is used to retain the predictive capability of the original model within the design space while mitigating computational costs. [13] In this study, Response Surface Models (RSM) of the SEL 80-dB noise exposure area and fuel burn were created as a function of the four operational variables and AEDT simulation results generated by the hybrid DoE. In order to evaluate the accuracy of the RSMs, a goodness of fit was performed with R^2 first.

Table 5. Goodness of fit (R^2)

	Fuel Burn	Noise Exposure Area
R^2	0.99717	0.98976
Adjusted R^2	0.99629	0.98657

Next, the Actual by Predicted plot was generated to determine how well the response is approximated by the model. As shown in Figure 6, the data points were evenly scattered along the perfect line and the points were quite close to the fit.

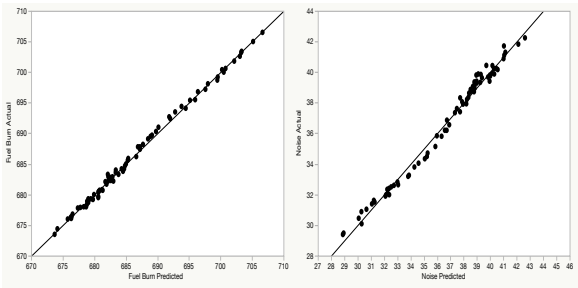

Figure 6. Actual vs. Predicted plot for noise and fuel burn

Finally, the errors of the RSMs were calculated by examining the distribution of the error for RSMs-produced data compared to the actual data. Since Model Fit Error (MFE) is a necessary but not sufficient as a measure of the accuracy of the Response model, 15 additional random DoE cases were simulated in AEDT and equivalently calculated using the surrogate model in order to evaluate Model Representation Error (MRE) to ensure the predictive capability of the response model. As a result, it was found that maximum error for fuel burn RSM was 0.17%; whereas, maximum error for noise exposure area was 2.16%. The mean of both fuel burn and noise exposure area were 0.000321 for fuel burn and 0.000756 for noise.

4.4. Monte-Carlo Simulations (MCS)

Using the generated RSMs of fuel burn and noise exposure area, MCSs was performed with

100,000 points to propagate the metrics of interest. In order to explore all operational factors and responses, both lower and upper limits of variables were used as the min/max values for uniform sampling distributions.

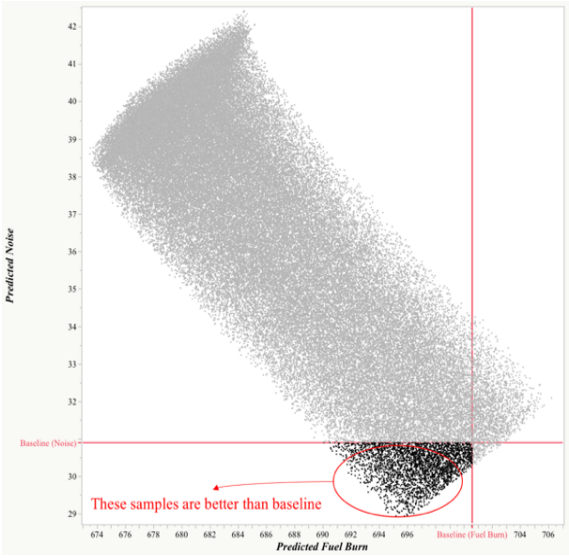

Figure 7. Monte-Carlo Simulations Results

As a result, it was found that there is an area where both noise and fuel burn are less than the baseline. In addition, a locus of points that is non-dominated was graphically captured, which indicated an inverse relationship between fuel burn and noise. However, since there is no guarantee that the points generated by MCS would be parsed at the Pareto front, Non-dominated Sorting Genetic Algorithm (NSGA) method [14] was implemented as shown in Figure 8.

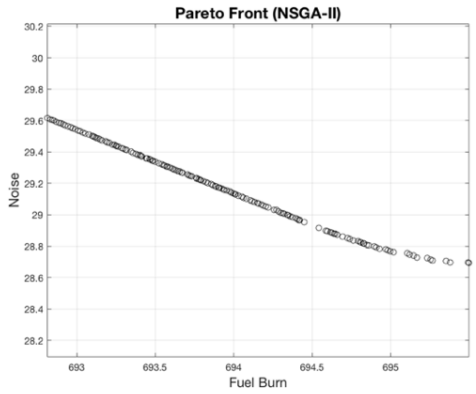

Figure 8. Pareto front generated by NSGA-II

4.5. Optimization Results

After investigating the RSM and MCS, it was found that the operational variable associated with takeoff thrust had the greatest influence on both noise and fuel burn as compared to other variables. The trends depicted in Figure 9 indicate that noise contour area decreases; whereas, fuel burn increases as the takeoff thrust is reduced. Furthermore, it shows that other operational variables have little impacts on both noise and fuel burn, due to the slight to moderate slopes.

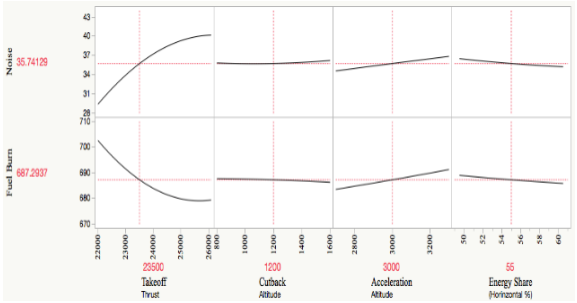

Figure 9. Prediction profiler

Since there is generally no optimal solution in a multi-objective optimization problem, two points representing each fuel burn and noise optimums on the Pareto front found by the NSGA-II were identified and run in AEDT to compare with the baseline.

Table 6. Baseline vs. Optimum (Aircraft-level)

Metric	Baseline	Noise Opt.	Fuel Burn Opt.
Noise Exp. Area (km^2)	30.9	29.4	29.9
Fuel used for flight (kg)	700.6	694.8	693.5
Takeoff Thrust (lbf)	22175.7	22175.7	22315.5
Cutback Altitude (ft)	1000	1140	1189
Acceleration Altitude (ft)	3000	2702	2721
Horizontal Acceleration (%)	55	60.5	60.5

As a result, the noise optimum case reduced SEL 80-dB noise exposure area (km^2) by approximately 5% and the fuel burn (in kilograms) optimum reduced by 1% relative to the baseline for the aircraft-level analysis. In Figure 10, dashed lines are optimized results and straight lines are baseline results. Red pin symbols indicate the specific measurement.

Figure 10. Baseline vs. Optimized (SEL noise exposure area)

5. Airport-Level Analysis

The next aspect of this investigation was to determine how the optimized procedure of Boeing 737-800 affected the noise exposure area and fuel burn metrics at the airport level. For airport-level analysis, the baseline case validated with the measurement data (March 20, 2017) was chosen and the optimized departure procedure of the Boeing 737-800 replaced all operations in the original flight schedule and the new schedule was executed in AEDT. As a result, the 75 WECPNL noise exposure area and total fuel used for the modified B737-800 flights decreased compared with the baseline case as tabulated in Table 7.

Table 7. Baseline vs. Optimum (Airport-level)

	Fuel Burn (kg)	WECPNL 75 dB (m^2)
Baseline	226,876	10,733,293
Optimization	226,542	10,727,508
Difference	0.2%	0.1%

While the difference between the baseline and optimum is quite small, this only reflects the optimization of the Boeing 737-800 departure procedure (89 out of 198 operations). It is expected that the 75 WECPNL noise exposure area would be further reduced when all departure aircraft are optimized. The optimized procedures should be verified with real flight experiments and this will be further investigated in future work.

6. Conclusion

In this study, an investigation was conducted on modeling different departure procedures at Gimpo International Airport. As the first step, verification and validation (V&V) for Gimpo International Airport were performed with the noise measurement data and the real flight operations. Preliminary results showed a good agreement overall, but small differences existed between simulation and measurement data due to unresolved discrepancies.

After the V&V was conducted, AEDT was executed with a variety of advanced design methods such as Design of Experiments (DoE), surrogate modeling, Monte-Carlo Simulations (MCS), and Pareto frontier analysis. Operational variables associated with Boeing 737-800 departure procedures were explored and four variables were finally chosen. For the DoE, 25 points were allocated for Central Composite Design (CCD) to capture corner points and 50 points were specified for Latin Hypercube Sampling (LHS) to capture interior points of the design space. For the 75 sample points, AEDT was run to generate results for fitting a surrogate model. In order to evaluate the surrogate model, goodness of fit was performed. Using the generated Response Surface Model (RSM) of fuel burn and noise exposure area, MCSs was performed with 100,000 points to propagate the metrics of interest. After investigating the RSMs and MCSs, it was found that the operational variable associated with takeoff thrust had the greatest influence on both noise and fuel burn metrics relative to the other variables. For the Pareto frontier analysis, a Non-dominated Sorting Genetic Algorithm (NSGA-II) method was implemented and it was found that fuel burn and noise were inversely related.

For aircraft-level analysis, two points representing the fuel burn and noise optimal cases on the Pareto front found by the NSGA-II were identified and run in AEDT to compare with the baseline. As a result, the noise optimum case reduced SEL 80-dB noise exposure area by approximately 5% and the fuel burn optimum case reduced by 1% relative to the baseline for an aircraft-level analysis.

Acknowledgement

The authors would like to thank Post-Doctoral Fellow Matthew LeVine for guidance and feedback on this study. The author also would like to thank Dr. Hyosung Sun (Korea Environmental Institute, KEI) for his support on the validation works in this study.

Student Biography

Junghyun Kim is a graduate research assistant at the Aerospace Systems Design Laboratory (ASDL) in Georgia Institute of Technology. Before he started to work for ASDL, he worked at Korea Aerospace Research Institute(KARI) in South Korea as a full-time researcher. He received his Master of Science in Aerospace Engineering from Seoul National University (SNU) and he graduated as top academic achievements student at the department of Aerospace Engineering from Sejong University (Summa Cum Laude). He has been sponsored by Korean government for studying abroad since 2015 and he is now pursuing a Ph.D. degree from Georgia Institute of Technology.

References

[1] Environmental Research and Consultancy Department, Civil Aviation Authority, "Aircraft noise and health effects: Recent findings" CAP 1278, 2016.

[2] Regional Office for Europe, World Health Organization, "Burden of Disease from environmental noise (Quantification of healthy life years lost in Europe)" ISBN: 978 92 890 0229 5, 2011.

[3] Federal Aviation Administration, "FAA Aerospace Forecast Fiscal Years 2017-2037", TC17-0002, 2017.

[4] IATA 20-year Passenger Forecast and Tourism Economics, "IATA Forecasts Paseenger Demand to Double Over 20 Years," Press Release No. 59, URL: http://www.iata.org/pressroom/pr/Pages/2016-10-18-02.aspx [cited 18 October 2016].

[5] Federal Aviation Administration, U.S. Department of Transportation, "Noise Abatement Departure Profiles", AC No: 91-53A, 1993.

[6] John-Paul Barrington Clarke, MIT, "System Analysis of Noise Abatement Procedures Enabled by Advanced Flight Guidance Technology," Journal of Aircraft, Vol. 37, No. 2, March-April 2000

[7] H.G. Visser and R.A.A.Wijnen, Delft University of Technology, "Optimization of Noise Abatement Departure Trajectories," Journal of Aircraft, Vol. 38, No. 4, July-August 2001

[8] Jung-Hon Son, Yeon-Myung Kim, Jin-Woo Park, Young-Ii Kim, The Korea Transport Institute, "A study on the Establishments of Aircraft Noise Abatement Procedures in Gimpo International Airport," Korea Noise Conference, KSNVE06A-21-01, 2006

[9] Federal Aviation Administration, "Integrated Noise Model," Policy, International affairs and Environment, URL: https://www.faa.gov/about/office_org/headquarters_offices/apl/research/models/inm_model/ [cited 23 June 2015].

[10] Federal Aviation Administration, "Aviation Environmental Design Tool – Technical Manual", OMB No. 0704-0188, March 2017.

[11] Aeronautical Information Publication, Republic of Korea, "Aerodrome location indicator and name", RKSS AD 2.1, September 2016.

[12] Taehyung Kim, Kyutae Kim, Jaehwan Kim, Soogab Lee, Seoul National University, "Conversion Relationship of Aircraft Noise Indices Between WECPNL and DENL," International Congress on Acoustics, August 2010

[13] Anthony A. Giunta, Sandia National Laboratory, "Overview of Modern Design of Experiments methods for Computational simulations," AIAA, AIAA 2003-0649, 2003.

[14] Korea Airport Corporation, Korean Government, "Noise countermeasure policy on Gimpo International Airport in 2012", Pamphlet 2012.

[15] Kalyanmoy Deb, IEEE Associate Member, "A fast and Elitist Multi-Objective Genetic Algorithm: NSGA-II," IEEE Transactions on Evolutionary Computation, Vol. 6, No. 2, April 2002.

[16] Federal Aviation Administration, "AEDT & Legacy Tools Comparisons", Released on June 3, 2016.

[17] Federal Aviation Administration, U.S. Department of Transportation, "Reduced and Derated Takeoff Thrust (Power) Procedures", AC No: 25-13, 1988.

[18] http://m.news.naver.com/read.nhn?mode=LSD&mid=sec&sid1=101&oid=421&aid=0002757577 [cited 29 May 2017].

[19] Federal Aviation Administration, U.S. Department of Transportation, "Environmental optimization of aircraft departures: Fuel burn, Emissions, and Noise", ACRP Report 86, 2013.

[20] John-Paul Barrington Clarke, Georgia Tech, "Optimized Profile Descent Arrivals at Los Angeles International Airport" Journal of Aircraft, March 2013.

[21] John-Paul Barrington Clarke, MIT, "Continuous Descent Approach: Design and Flight Test for Louisville International Airport" Journal of Aircraft, September 2004.

[22] Tom G. Reynolds and John-Paul Barrington Clarke, University of Cambridge and Georgia Tech, "History, Development and Analysis of Noise Abatement Arrival Procedures for UK Airports" 5th AIAA Aviation Technology, September 2005.